MATERIALE PLASTICE
https://revmaterialeplastice.ro
https://doi.org/10.37358/Mat.Plast.1964

Performance Assessment of HMAM under Different Climate Zones Using a Multi-Criteria Decision Approach

HUAIZHI ZHANG[1], WENNAN AN[1*], BINCHENG GU[2], JINCHANG WANG[3]
[1] School of Transportation and Geomatics Engineering, Shenyang Jianzhu University, Shenyang, China
[2] Second Construction Limited Company of China Construction Eighth Engineering Division, Jinan, China
[3] Institute of Transportation Engineering, Zhejiang University, Hangzhou, China

Abstract: ***Purpose:*** *This study investigates the comprehensive performance of high-modulus asphalt mixtures (HMAM) with a focus on their climate-specific suitability, which is insufficiently addressed in existing research.* ***Methodology:*** *Four asphalt mixtures—70-penetration asphalt, styrene–butadiene–styrene (SBS)-modified asphalt, HMAM-Lubao, and HMAM-H7686—were evaluated using wheel-tracking (rutting), low-temperature bending, water stability, and uniaxial compression tests. An improved analytic hierarchy process (AHP) was applied to assign indicator weights across different climate zones.* ***Findings:*** *HMAMs exhibited superior rutting resistance, water stability, and modulus compared with conventional and SBS-modified mixtures. Among them, HMAM-H7686 ranked highest in hot and rainy zones, while HMAM-Lubao demonstrated more balanced performance in colder climates.* ***Value:*** *This study establishes an adaptable and transparent evaluation framework by integrating multi-index laboratory testing with an improved AHP method. The framework provides practical guidance for selecting asphalt mixtures according to climate zones, supporting more durable pavement design and construction.*

Keywords: *Pavement engineering, analytic hierarchy process, high-modulus asphalt mixture, climate adaptation, performance evaluation, polymer modification, composite materials, material characterization*

1. Introduction

Asphalt pavements experience gradual structural degradation over time due to the cumulative effects of environmental factors and traffic loading, resulting in various forms of distress. As a common and recurrent distress, rutting manifests as continuous longitudinal plastic deformation along the wheel paths. It not only markedly impairs ride comfort and traffic safety, but also induces stress concentrations that accelerate crack propagation and secondary distresses such as moisture damage, ultimately shortening pavement service life. Research demonstrates that enhancing the overall performance of asphalt mixtures effectively mitigates permanent deformation [1–5]. High-modulus asphalt mixtures (HMAM) originated in France, where the high-modulus asphalt concrete standard NF P98-140 was established. Since then, HMAM has attracted increasing attention in pavement engineering. In this study, high-modulus asphalt mixtures (HMAM) are defined as asphalt mixtures whose stiffness modulus is significantly higher than that of conventional dense-graded mixtures, typically achieved through the incorporation of high-modulus modifiers. In China, HMAM are produced by directly integrating high-modulus modifiers into an aggregate matrix. HMAM has proven effective in middle-layer applications for heavy traffic [6]. International practice on HMAM/EME provides benchmarks for performance expectations [7,8]. This approach significantly enhances the resistance of the mixture to various types of deformation. In practice, pavement performance is primarily evaluated using dynamic stability, bending failure strain, water stability, and other parameters specified in the *Technical Specifications for Construction of Highway Asphalt Pavements (JTG F40-2004)*. Given the substantial climatic

email: an571120078@foxmail.com

variations across the different regions of China, the suitability of asphalt mixtures varies. Moreover, a comprehensive and scientifically grounded evaluation system for mixture selection across different climates is still lacking. It is essential to study the selection methods for asphalt mixtures based on various performance indicators and climate zones [9–12].

A growing consensus in pavement engineering acknowledges the critical role of high stiffness in mitigating rutting, propelling research into High-Modulus Asphalt Mixtures (HMAM) as a promising solution. Head-to-head tests indicate that the two HMAM formulations assessed here deliver across-the-board gains over conventional mixes, reflecting the influence of the high-modulus additive [13,14]. A DXG-2 high-modulus modifier was used to elevate the modulus of the conventional asphalt mixtures. Tests were conducted to assess splitting strength, static resilient modulus, and dynamic modulus. The results demonstrated that increasing the modifier content significantly improved the splitting strength of the asphalt mixture [15]. Road performance tests provide a direct means of evaluating the engineering properties of asphalt mixtures. However, a comprehensive assessment system that includes rutting resistance and water stability derived from road performance testing results is essential.

Saaty proposed the Analytic Hierarchy Process (AHP), a straightforward multi-criteria method for quantifying qualitative issues [16–18]. This method has been refined through research and successfully applied across various engineering domains. We construct an integrated multi-criteria framework for slope stability by fusing group decision-making theory, AHP, and a fuzzy comprehensive evaluation scheme [19]. The post-assessment indicator system for cold recycling technology projects was established based on AHP, and the weights for various factors were calculated [20,21]. Using a model developed by researchers based on three key indicators: void ratio, stability, and flow, the weight coefficients for each evaluation parameter were determined, along with the optimal combination of aggregate and binder/aggregate ratios [22–24]. A more scientific and reasonable comparative scale, Table 5/5–9/1, was adopted to support the AHP, indicator weights were determined via AHP to balance multi-performance criteria [25]. The results indicate that the improved AHP features straightforward models that are easy to understand and can be utilized to optimize water-saving irrigation methods [26].

The Analytic Hierarchy Process (AHP) has been extensively applied to various engineering problems. However, a performance evaluation system for asphalt mixtures that explicitly accounts for different climate zones is still lacking. In this study, the four asphalt mixtures were first subjected to a full set of road performance tests. Based on these results, a comprehensive evaluation framework was established, incorporating indicators such as high-temperature performance, low-temperature performance, moisture resistance, and temperature sensitivity. An AHP-based weighting method was then used to assign weight coefficients to each indicator. This approach enables the calculation of overall performance scores for different asphalt mixtures across multiple climate zones, thereby supporting more systematic and transparent material selection.

This study presents two core novel contributions to the understanding and application of High-Modulus Asphalt Mixtures (HMAMs). First, we provide a climate-aware quantitative performance benchmarking of two commercial HMAM formulations, H7686 and Lubao, across various climate zones, allowing engineers to make more informed material selection based on specific climate needs. Second, we conduct a quantitative validation of HMAM adaptability across multi-climate zones by integrating multi-index test data with climate-specific weights, generating comprehensive performance scores that quantify the suitability of HMAMs for diverse environments.

2. Materials and aggregate gradation

2.1. Material

All mixes employed a 70-pen asphalt binder compliant with JTG F40—2004. The supplier's technical data are summarized in Table 1. Limestone served as the aggregates.

Table 1. Properties of 70-penetration asphalt

Properties	Unit	Value	Method
Penetration (25°C, 100 g, 5 s)	0.1 mm	63.2	T0604
Softening Point	°C	49.1	T0606
Ductility (5 cm/min, 15°C)	cm	>100	T0605
Viscosity (177°C)	Pa·s	3.8	T0625-2011

This study employed two high-modulus modifiers, Honeywell 7686 (H7686) and Lubao, chosen for proven efficacy and operational simplicity (Figure 1). During mixture production, the modifiers were incorporated via the dry process, i.e., directly mixed with the aggregates.

(**a**) (**b**)

Figure 1. High modulus modifiers: (a) Honeywell7686; (b) Lubao

Honeywell 7686 is a white powder and low molecular weight composite that is soluble in asphalt. This modifier offers improved rutting and water resistance, making it suitable for warm-mixing applications. Lubao, a high-density polyethene, exhibits excellent chemical stability, a high molecular weight, and is odorless and nontoxic. Its incorporation into asphalt mixtures enhances overall performance. The characteristics of H7686 and Lubao are presented in Tables 2 and 3, respectively.

Table 2. Properties of H7686

Properties	Method	Value
Droplet Point	SH/T 0800-2007	130°C–138°C
Viscosity—150°C Brookfield	SH/T 0739-2003	4.1–4.8 Pa·s

Table 3. Properties of Lubao

Properties	Value	Standards
Tensile strength/MPa	18.8	18~20
Elongation at break/%	102.8	≥100
Density/(g.cm^{-3})	0.94	0.93~0.96
Melt flow rate/(g/10 min)	1.2	1~4
Vicat softening temperature/°C	61.7	≤140
Resin content/%	98.89	≥95
Particle diameter/mm	3.7	3~5

2.2. Aggregate gradation

The gradation adopted was AC-20. This is a dense-graded hot-mix asphalt with a nominal maximum aggregate size of 20 mm. Its mineral particle gradation, designed based on the dense gradation concept, adheres to the Chinese standard "JTG F40—2004". Gradation and indicator weights were optimized using fuzzy-AHP [27]. The continuous aggregate gradation (with a nominal maximum size of 19 mm) is presented in Table 4.

Table 4. Gradation

Sieve size/mm	26.5	19	16	13.2	9.5	4.75	2.36	1.18	0.6	0.3	0.15	0.075
Upper limit/%	100	100	92	80	72	56	44	33	24	17	13	7
Lower limit/%	100	90	78	62	50	26	16	12	8	5	4	3
Gradation/%	100	93.7	86.3	79.2	66.3	45.9	28.1	20.0	13.2	8.1	5.4	3.6

Mixtures were proportioned with the Marshall method using 70-pen and SBS binders, yielding an optimum asphalt content of 4.4% for both conventional mixes. High-modulus additives were then introduced at supplier-specified dosages (H7686: 0.4%; Lubao: 0.5% of total mixture mass) by dry addition to the aggregates. The optimized binder contents increased to 4.5% (H7686) and 4.6% (Lubao). Mixing was performed at 160 Â°C for 90 min, low-temperature performance was evaluated with multi-index criteria [28–32].

Asphalt mixtures using a 70-penetration asphalt binder are referred to as Asphalt Mix 70-penetration. Similarly, those incorporating an SBS asphalt binder were designated as Asphalt Mix-SBS. For the high-modulus modified asphalt mixtures, those modified with Lubao were specifically termed HMAM-Lubao, whereas those modified with H7686 were designated HMAM-H7686. These distinct nomenclatures are essential for the precise identification and differentiation of asphalt mixtures in research and practical applications. Each mixture possessed unique characteristics and performance properties that were directly related to the binder or modifier used. For instance, HMAM-Lubao may demonstrate superior performance owing to the addition of Lubao, and the naming convention helps researchers and engineers quickly comprehend the mixture composition and predict its potential performance.

3. Experimental procedures and analysis

The experimental design followed the standard testing procedures outlined in JTG E20-2011. The specimen quantities used for each test were 3 specimens for rutting, 6 specimens for bending, 6 specimens for water stability, and 3 specimens for modulus testing at each temperature level. This ensures that the data presented in this study are both consistent with established testing norms and reliable for performance evaluation across various climatic conditions.

3.1. Wheel rutting test

Dynamic stability directly reflects the rutting resistance of asphalt pavements and is positively correlated with the high-temperature rut resistance. A rut board measuring 300 × 300 × 50 mm was meticulously fabricated using a hydraulic sample-forming machine, as illustrated in Figure 2. This hydraulic machine was selected because of its precision in producing uniform and accurately sized samples, thereby ensuring reliability of the test results. The rutting test, which is a critical procedure for evaluating the performance of asphalt materials, was conducted using a specialized rutting apparatus under a standard wheel load of 780 N. The test was performed at 60°C, which is the standard temperature chosen to simulate the high-temperature conditions commonly encountered by asphalt pavements in real-world applications [33]. Performance is jointly affected by high temperature and moisture during rainy seasons [34–36]. Fatigue resistance trends were evaluated under multiple stress levels [37]. This

temperature plays a significant role in influencing the rutting behavior of asphalt mixtures. HMAM demonstrated superior rutting resistance and higher modulus across temperatures. The detailed results from this rutting test are presented in Table 5, enabling a comprehensive analysis and comparison of the rutting performances of various asphalt mixtures.

Figure 2. Rutting test

Table 5. Results of rutting tests (mean ± standard deviation, with CV in parentheses)

Sample description	45 min rut depth/mm	60 min rut depth/mm	DS/(times·mm^{-1})	Relative deformation ratio/%	n
Asphalt mix-70 penetration	3.781 ± 0.23 (6.1%)	4.182 ± 0.25 (6.0%)	1571 ± 110 (7.0%)	8.36 ± 0.55 (6.6%)	3
Asphalt mix-SBS	2.160 ± 0.11 (5.1%)	2.303 ± 0.12 (5.2%)	4405 ± 260 (5.9%)	4.61 ± 0.28 (6.1%)	3
HMAM-Lubao	1.403 ± 0.07 (5.0%)	1.501 ± 0.08 (5.3%)	6428 ± 310 (4.8%)	3.00 ± 0.18 (6.0%)	3
HMAM-H7686	0.680 ± 0.03 (4.4%)	0.739 ± 0.04 (5.4%)	10,857 ± 615 (5.7%)	1.48 ± 0.09 (6.1%)	3

As shown in Table 5, the high-temperature performance of the two HMAM types significantly surpassed that of conventional asphalt mixtures. Specifically, the dynamic stability of HMAM-H7686 increased seven-fold compared with that of the base asphalt, and HMAM-Lubao exhibited a fourfold improvement. Additionally, HMAM-H7686 demonstrated superior high-temperature resistance compared to HMAM-Lubao, with a 2.5-fold performance enhancement relative to that of the SBS-modified asphalt mixture.

While adjusting binder content is important for a fair comparison, the H7686 and Lubao modifiers play a crucial role in enhancing the mixture's stiffness and thermal stability, leading to better rutting resistance and low-temperature cracking resistance. Although increasing binder content can improve rutting resistance, the improvements observed in this study were primarily due to the modifiers, not just the binder content. This highlights the significant contribution of H7686 and Lubao in enhancing the performance of high-modulus asphalt mixtures.

3.2. Bending test at low temperature

To evaluate the low-temperature performance of the HMAM, track plate specimens made by wheel rolling were cut into 250 × 30 × 35 small beams following the standard test method (JTG E20—2011) [33]. As shown in Figure 3, the effective beam span is 200 mm. The bending failure tests were performed at −10°C, and the results are listed in Table 6.

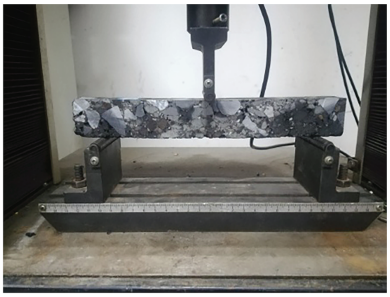

Figure 3. Bending failure test

Table 6. Results of bending failure strain tests (mean ± standard deviation, with CV in parentheses)

Sample description	Bending failure strain/με	n
Asphalt mix-70 penetration	2376 ± 155 (6.5%)	3
Asphalt mix-SBS	2816 ± 170 (6.0%)	3
HMAM-Lubao	2611 ± 145 (5.6%)	3
HMAM-H7686	2398 ± 130 (5.4%)	3

As shown in Table 6, Asphalt mix-SBS had the best low-temperature performance, followed by HMAM-Lubao, and Asphalt mix-70 penetration had the worst performance.

3.3. Water stability test

In this study, one freeze–thaw splitting test was adopted primarily for baseline comparison and preliminary screening among different asphalt mixtures, in accordance with the current Chinese standard (JTG E20-2011, T0709, T0716). Immersion, Marshall, and freeze-thaw splitting tests were conducted at a controlled temperature of 20°C to evaluate the water resistance of the materials. These tests were conducted in strict accordance with the standard test method [33]. The procedures and guidelines outlined in this standard ensure the reliability and comparability of test results. Following these protocols, the residual stability and freeze-thaw splitting strength ratios were calculated. As shown in Figure 4, these calculated ratios are key indicators for assessing the water resistance of materials. The water resistance of asphalt mixtures is vital because it directly affects the durability and service life of road pavement. The test results provide valuable insights into the water-resistance performance of the materials and are presented in Figure 5. This graphical presentation facilitates straightforward analysis and comparison of the water-resistance characteristics of the different mixtures.

(**a**) (**b**)

Figure 4. Water stability tests: (a) stability test and (b) freeze-thaw splitting test

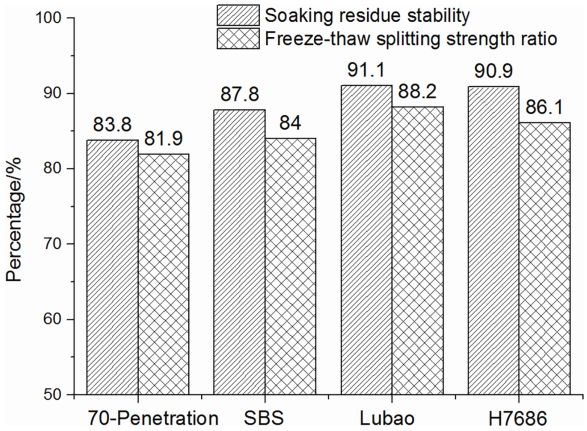

Figure 5. Water stability results

As shown in Figure 5, the residual stability and TSR (Tensile Strength Ratio) values of the two HMAM were higher, followed by those of the asphalt mix-SBS. This indicates that a high-modulus modifier can enhance the water resistance of asphalt mixtures. Therefore, it is advisable to promote the use of High-Modulus Asphalt Mixtures (HMAM) in the high-temperature and rainy regions of southern China.

3.4. Uniaxial compression tests

Uniaxial compression tests were performed to determine the static moduli of the four asphalt mixtures. Previous research has suggested that these specimens are cylindrical or nearly cube-shaped prisms. Because an optimal height-to-diameter ratio of 2 was ideal for the specimens, each beam was cut into 40 × 40 × 80 mm prism specimens, as shown in Figure 6. This specimen size was selected to minimize size effects on the measured mechanical response. The test temperatures were set at 5°C, 15°C, 20°C, 30°C, 45°C, and 60°C, with a loading rate of 50 mm/min [33]. The temperature was gradually increased to the target value after the specimen was placed in the environmental chamber. The specimens were conditioned for at least 4 h to ensure a thermal equilibrium. This long conditioning time was crucial because it allowed the specimen to fully adapt to the set temperature, ensuring more accurate test results. By carefully controlling these parameters, a uniaxial compression test can effectively measure the static modulus of asphalt mixtures under various temperature conditions.

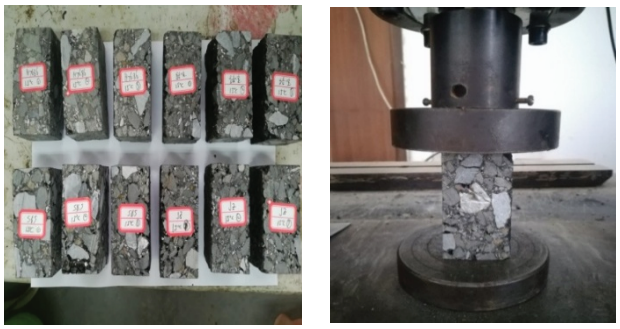

(**a**) (**b**)

Figure 6. Uniaxial compression tests: (a) test specimens and (b) modulus test. Note: 1. The three samples in the top-left: HMAM-H7686 at 15°C; 2. The three samples in the top-right: HMAM-Lubao at 15°C; 3. The three samples in the bottom-left: Asphalt mix-SBS;4. The three samples in the bottom-right: Asphalt mix-70 penetration at 15°C.

The compressive strengths of the asphalt mixtures were calculated based on test results. Then, the static modulus was computed according to the compressive strength and linear deformation of the straight stage of the load-deformation curve. The static moduli are listed in Table 7.

As shown in Table 7, the various asphalt mixtures were highly sensitive to temperature, and the static modulus was negatively correlated with the temperature. The moduli of both HMAM increased.

Table 7. Static modulus test results at different temperatures (mean ± standard deviation, with CV in parentheses)

Temperature/°C	5	15	20	30	45	60
Sample description	**Average static modulus/MPa**					
Asphalt mix-70 penetration	1366 ± 82 (6.0%)	1016 ± 61 (6.0%)	838 ± 50.3 (6.0%)	474 ± 28.4 (6.0%)	92 ± 5.5 (6.0%)	68 ± 4.1 (6.0%)
Asphalt mix-SBS	1402 ± 70.1 (5.0%)	1192 ± 59.6 (5.0%)	994 ± 49.7 (5.0%)	498 ± 24.9 (5.0%)	134 ± 6.7 (5.0%)	96 ± 4.8 (6.5%)
HMAM-Lubao	2632 ± 105.3 (4.0%)	2148 ± 85.9 (4.0%)	1872 ± 74.9 (4.0%)	796 ± 31.8 (4.0%)	284 ± 11.4 (4.0%)	132 ± 5.3 (4.0%)
HMAM-H7686	2470 ± 155 (3.8%)	2006 ± 76.2 (3.8%)	1826 ± 69.4 (3.8%)	846 ± 32.1 (3.8%)	378 ± 14.4 (3.8%)	186 ± 7.1 (3.8%)

4. Comprehensive performance evaluation of asphalt mixture

4.1. Comparative matrix method in AHP

AHP is a qualitative and quantitative method developed by American operational analyst Saaty [38]. The comparative matrix in AHP determines the weight coefficients of the performance indicators. The comparative matrix in AHP determines the weight coefficients of the performance indicators. The selected evaluation indicators included the high- and low–temperature performance, water resistance, and temperature sensitivity. Relative degree factors were determined based on high and low temperatures, precipitation, and temperature differences across various climate zones, and the weights of the corresponding evaluation elements were established. For practical interpretation, representative cities can be associated with the climatic zones used in this study. used in qualitative or survey-based decision-making, in this study it was adapted to continuous laboratory data. The raw test results of each performance indicator were first normalized and converted into dimensionless graded scores according to specification limits and engineering practice, and these scores were subsequently used in the AHP evaluation process. The core concept involves constructing a comparison matrix based on the relative significance of indicators. Eigenvectors can be derived from this matrix to determine the weight coefficients. There are four steps to follow when addressing problems using AHP [39–42].

(1) Establishment of the structural hierarchy model

The goals and factors of each model are plotted against each other. To determine the overall evaluation indicator U, $U = (u_1, u_2, ..., u_n)$, four indicators were used in this study: high temperature, low temperature, water resistance, and temperature sensibility performance. Therefore, $n = 4$. The importance of the high-temperature performance compared with other properties was considered as a benchmark. The comparative matrix model is presented in Table 8.

Table 8. Comparative matrix model

Climate zones	High-temperature performance	Low temperature performance	Water resistance performance	Temperature-sensitivity performance
High temperature performance	1	High/Low temperature importance degree	High temperature/ Water resistance importance degree	High temperature/ Temperature-sensibility importance degree
Low temperature performance		1	Low temperature/Water resistance importance degree	Low temperature/ Temperature-sensibility importance degree
Water resistance performance			1	Water resistance/ Temperature-sensibility importance degree
Temperature-sensibility performance				1

(2) Determination of matrix scale

When the *i*-th element is compared with the importance of the *j*-th factor, the quantified relative weight a_{ij} is used to describe the importance of each factor to the *i*-th element. The current scale is primarily based on the 1–9 scale proposed by Saaty. Although this method is widely used owing to its coarser scale, the importance of an element is easily amplified when the performance is compared, and the evaluation result is not sufficiently objective. Based on the above situation, the 5/5–9/1 judgment matrix had the least deviation and was more in line with the objective reality [43]. Hence, the improved 5/5–9/1 scale and the coefficients of relative importance were used as standards, as shown in Table 9.

Table 9. Improved comparison matrix scale (5/5–9/1)

Relative importance	Definition-specification	Element *i* is higher than element *j* grade
5/5 = 1.00	Equal importance	0
6/4 = 1.50	Slightly important	1
7/3 = 2.33	More important	2
8/2 = 4.00	Very important	3
9/1 = 9.00	Absolute important	4
5.5/4.5, 6.5/3.5, 7.5/2.5, 8.5/1.5	It needs to be used when compromised	/

(3) Comparison of matrix constructions

A matrix model can be constructed based on the degree of difference between a benchmark and the other indicators. In this study, the high-temperature performance was used as a benchmark to calculate other coefficients, specifically $r_{i,i} = 1$, and these coefficients were referenced using the benchmark performance. In the first row, the matrix must be determined based on the relative importance of high-temperature performance and other performances. For $r_{2,3}$ in the second row, $r_{1,3}/r_{1,2}$ are required, and

the importance of low temperature relative to the water resistance can be obtained. The coefficient, that is, the other half matrix, can be drawn according to $r_{i,j} = 1/r_{j,i}$. The comparison matrix is established as follows:

$$R = \begin{bmatrix} r_{11} & \cdots & r_{1n} \\ \vdots & \ddots & \vdots \\ r_{n1} & \cdots & r_{nn} \end{bmatrix} \quad (1)$$

(4) Comparison of matrix consistency checks.

Consistency pertains to logical coherence among the evaluation indicators. For instance, if A is more crucial than C and B is somewhat more critical than C, then, logically, A must be more important than B. This represents the logical consistency between the evaluation indicators. If this consistency is not met, there is an issue with the judgment. The consistency ratio *CI* is computed to conduct a consistency check. Initially, the consistency indicator is defined as:

$$CI = \frac{\lambda_{max} - n}{n - 1} \quad (2)$$

where λ_{max} represents the maximum eigenvalue and n denotes the matrix order. When $CI = 0$, it indicates a high degree of consistency; conversely, the larger the value of *CI*, the more inconsistent the situation. Subsequently, *CR* was calculated as follows:

$$CR = \frac{CI}{RI} \quad (3)$$

where *RI* is a random consistency indicator, and its values are listed in Table 10. When *CR* was <0.1, the level of inconsistency was within the acceptable range.

Table 10. Random consistency indicator (*RI*)

n	**1**	**2**	**3**	**4**	**5**	**6**	**7**	**8**	**9**	**10**
RI	0	0	0.58	0.90	1.12	1.24	1.32	1.41	1.45	1.49

High- and low-temperature performance grades as well as corresponding climate zones were considered. The temperature difference grade was divided into three grades: large, medium, and small temperature difference zones. Based on the range of high temperatures, the temperature performance was classified into grades 1, 2, and 3. Initially, in line with the "Technical Specifications for Construction of Highway Asphalt Pavements (JTG F40—2004)" in China, the descriptions of the performance indicators are presented in Tables 11–14.

Table 11. Description of high-temperature grades

High-temperature grades	**1**	**2**	**3**
Maximum average monthly maximum temperature/°C	>30	20~30	<20

Table 12. Description of low-temperature grades

Low-temperature grades	1	2	3	4
Extreme minimum temperature/°C	<−37.0	−37.0~−21.5	−21.5~−9.0	>−9.0

Table 13. Description of precipitation grades

Precipitation grades	1	2	3	4
Annual rainfall/mm	>1000	1000~500	500~250	<−250

Table 14. Description of temperature difference grades

Temperature difference grades	1	2	3
Temperature difference/°C	51.5~67	39~51.5	<39

Six climate zones were selected from south to north, according to the climate zone map of China. Owing to space limitations, the weight coefficients in the other zones were not presented. A summary of the indicator grades is presented in Table 15.

Table 15. Summary of performance indicator grades for different climate zones

Climate zones	High temperature grade	Low temperature grade	Precipitation grade	Temperature difference grade
1-2-4	1	2	4	1
1-3-2	1	3	2	2
1-4-1	1	4	1	3
1-4-2	1	4	2	3
2-1-3	2	1	3	1
2-2-2	2	2	2	2

For example, Lianyungang and Xi'an can be regarded as representative cities for Zone 1-3-2, while Shenyang is representative of Zone 2-2-2. These examples help link the abstract climatic classification to real-world engineering environments and provide clearer guidance for HMAM application.

4.2. Computation of weight coefficients using the comparative matrix method

Based on the performance difference of indicators for each climate zone, a modified 5/5–9/1 scale was used, and the comparison matrix was established by referring to the assignment method in the third step of Section 4.1. Comparison matrices for the six zones were established, as shown in Figure 7.

The eigenvectors and maximum eigenvalues were normalized to the solution of the matrices as follows:

$\omega_{1\text{-}2\text{-}4} = (0.343, 0.229, 0.086, 0.343)\text{T}, \lambda_{max} = 4.0003$
$\omega_{1\text{-}3\text{-}2} = (0.362, 0.155, 0.241, 0.241)\text{T}, \lambda_{max} = 4.0002$
$\omega_{1\text{-}4\text{-}1} = (0.373, 0.093, 0.373, 0.160)\text{T}, \lambda_{max} = 4.0004$
$\omega_{1\text{-}4\text{-}2} = (0.426, 0.107, 0.284, 0.183)\text{T}, \lambda_{max} = 4.0001$
$\omega_{2\text{-}1\text{-}3} = (0.214, 0.322, 0.143, 0.321)\text{T}, \lambda_{max} = 4.0000$
$\omega_{2\text{-}2\text{-}2} = (0.250, 0.250, 0.250, 0.250)\text{T}, \lambda_{max} = 4.0000$

$$\begin{bmatrix} 1 & 1.5 & 4 & 1 \\ 1.5 & 1 & 1.55 & 0.667 \\ 0.25 & 0.645 & 1 & 0.429 \\ 1 & 1.5 & 2.33 & 1 \end{bmatrix} \quad \begin{bmatrix} 1 & 2.33 & 1.5 & 1.5 \\ 0.429 & 1 & 0.644 & 0.644 \\ 0.667 & 1.553 & 1 & 1 \\ 0.667 & 1.553 & 1 & 1 \end{bmatrix}$$

(a) **(b)**

$$\begin{bmatrix} 1 & 4 & 1 & 2.33 \\ 0.25 & 1 & 0.25 & 0.5825 \\ 1 & 4 & 1 & 2.33 \\ 0.429 & 1.717 & 0.429 & 1 \end{bmatrix} \quad \begin{bmatrix} 1 & 4 & 1.5 & 2.33 \\ 0.25 & 1 & 0.375 & 0.5825 \\ 0.667 & 2.667 & 1 & 1.553 \\ 0.429 & 1.717 & 0.644 & 1 \end{bmatrix}$$

(c) **(d)**

$$\begin{bmatrix} 1 & 0.667 & 1.5 & 0.667 \\ 1.5 & 1 & 2.25 & 1 \\ 0.667 & 0.444 & 1 & 0.444 \\ 1.5 & 1 & 2.25 & 1 \end{bmatrix} \quad \begin{bmatrix} 1 & 1 & 1 & 1 \\ 1 & 1 & 1 & 1 \\ 1 & 1 & 1 & 1 \\ 1 & 1 & 1 & 1 \end{bmatrix}$$

(e) **(f)**

Figure 7. Comparison matrices for different climate zones: (a) 1-2-4; (b) 1-3-2; (c) 1-4-1; (d) 1-4-2; (e) 2-1-3; (f) 2-2-2

After the consistency test, it was determined that the CR satisfied these requirements. The recommended weight coefficients for the asphalt mixtures in different climate zones are listed in Table 16.

Table 16. Recommended weight coefficients

Climate zones	High temperature performance weights	Low temperature performance weights	Water stability performance weights	Temperature sensitivity performance weights
1-2-4	0.343	0.229	0.086	0.343
1-3-2	0.362	0.155	0.241	0.241
1-4-1	0.373	0.093	0.373	0.160
1-4-2	0.426	0.107	0.284	0.183
2-1-3	0.214	0.322	0.143	0.321
2-2-2	0.250	0.250	0.250	0.250

CI/CR values per climate zone are presented in Table 17, alongside a short sensitivity analysis on the weight coefficients.

Table 17. Consistency index (CI), consistency ratio (CR), and comparison matrices per climate zone

Climate zones	CI	RI	CR	Consistency status
1-2-4	0.0003/3	0.9	0.0003/(3 × 0.9)	Meets requirement (CR < 0.1)
1-3-2	0.0002/3	0.9	0.0002/(3 × 0.9)	Meets requirement (CR < 0.1)
1-4-1	0.0004/3	0.9	0.0004/(3 × 0.9)	Meets requirement (CR < 0.1)
1-4-2	0.0001/3	0.9	0.0001/(3 × 0.9)	Meets requirement (CR < 0.1)
2-1-3	0	0.9	0	Perfect consistency
2-2-2	0	0.9	0	Perfect consistency

As shown in Table 17, all values are below the threshold of 0.1, ensuring that the consistency is acceptable for all zones.

Weight sensitivity analysis based on the 1-2-4 zone is summarized in Table 18.

Table 18. Sensitivity analysis on weights

Scenario	High temperature performance weights	Low temperature performance weights	Water stability performance weights	Temperature sensitivity performance weights	Ranking of mixtures	Max score difference
Base scenario (Original Weights)	0.35	0.20	0.10	0.35	HMAM-H7686 > HMAM-Lubao > 70# Mix > 50# Mix	0.032
Scenario 1: +10% High temperature	0.385	0.19	0.09	0.317	Same ranking as base	0.030
Scenario 2: −10% High temperature	0.315	0.21	0.11	0.365	Same ranking as base	0.031
Scenario 3: +10% Low temperature	0.345	0.22	0.09	0.345	Same ranking as base	0.034
Scenario 4: −10% Low temperature	0.355	0.18	0.11	0.355	Same ranking as base	0.034

As shown in Table 18, the results demonstrate that the rankings remain stable, with minimal variations in the score differences. In the table, 70# Mix refers to 70# Matrix Asphalt Mixture.

4.3. The score of the indicators

The indicators were categorized into four grades: excellent, good, medium, and qualified, with values of 9, 8, 7, and 6, respectively. The intervals between adjacent indicator grades were determined independently. Baseline criteria were set to the minimum thresholds in JTG F40—2024 (*Technical Specifications for Construction of Highway Asphalt Pavements*). High-temperature behavior was evaluated using the dynamic stability index. This indicator is crucial because it reflects the extent to which asphalt pavements can resist deformation under high-temperature and repeated-load conditions, which is vital for maintaining the smoothness and durability of the road surface in hot weather. The maximum failure strain determines the low-temperature performance. At low temperatures, asphalt mixtures are prone to cracking. The maximum failure strain indicates the ability of a material to withstand tensile stress before breaking, thereby indicating its resistance to temperature cracking. The water resistance was evaluated using two key parameters: residual stability and splitting strength ratio. The residual stability measures the ability of an asphalt mixture to maintain its integrity after immersion in water. The splitting strength ratio reflects the effect of water on the tensile strength of a mixture. These two aspects comprehensively assess the ability of asphalt pavements to withstand water-related damage such as stripping and softening, which are common problems in wet environments.

Temperature is a crucial factor that influences the mechanical properties of mixtures. Therefore, in the classification of temperature-sensibility properties, two parameters used in pavement structure design were considered. Specifically, the rate of change of the modulus from 15°C to 20°C was adopted as an indicator. The lower the modulus change rate, the stronger is the resistance to temperature differences. The rate of change of the modulus can be calculated as follows:

$$\nu = \frac{E_{15} - E_{20}}{E_{15}} \tag{4}$$

To ensure the robustness of this temperature-sensibility indicator, additional analyses were conducted to validate its applicability across broader temperature ranges, and the key findings are as follows:

Rationale for selecting the 15°C–20°C interval. The 15°C–20°C temperature interval was chosen because it closely matches the most common temperature conditions for asphalt pavements in real-world climates, particularly during the transitional seasons (spring and autumn) in most of the climatic zones considered in this study. This range represents the temperature variation that affects the modulus of asphalt mixtures under typical operational conditions, where subtle changes in temperature are more likely to impact long-term pavement performance. The temperature sensitivity evaluated in this range avoids the extreme effects observed at lower (<5°C) or higher (>30°C) temperatures, where the material behavior is significantly different (e.g., phase transitions or softening) and outside the intended scope of this analysis. Thus, the 15°C–20°C interval provides a more stable and representative measure of the temperature sensitivity for practical engineering applications.

Validation across a broader temperature range. We have extended our analysis to the full temperature range (5°C–60°C), as shown in the supplementary materials. The results indicate that the relative rankings of the mixtures (in terms of temperature sensitivity) remain consistent across the full temperature range. However, using the full range includes extreme temperatures that are already evaluated by other indicators, such as low-temperature strain and high-temperature dynamic stability. The use of 15°C–20°C focuses specifically on the subtle modulus changes within typical service conditions, making it a more focused and practical metric for long-term pavement performance under normal operating temperatures.

Consistency of core conclusions. As shown in Tables 19 and 20 (Supplementary Data), the rankings of the mixtures, based on the 15°C–20°C modulus change rate, were found to be consistent with those based on the full-range modulus temperature coefficient (MTC). This demonstrates that the conclusions drawn from the 15°C–20°C interval hold true when applying a broader slope/fit across the full temperature range, ensuring the robustness of the results.

Table 19. Full-range modulus slope calculation and sensitivity ranking

Sample description	MTC (MPa/°C)	R^2 of linear fit	Sensitivity ranking (full range)	Sensitivity ranking (15°C–20°C)
Asphalt mix-70 penetration	−31.2	0.92	4 (Most Sensitive)	4
Asphalt mix-SBS	−28.7	0.94	3	3
HMAM-Lubao	−22.5	0.95	2	2
HMAM-H7686	−19.8	0.96	1 (Least Sensitive)	1

Table 20. Impact of full-range sensitivity on comprehensive performance rankings

Climate zone	Original top-ranked mixture	Updated top-ranked mixture	Consistency
1-2-4	HMAM-H7686	HMAM-H7686	100%
1-3-2	HMAM-H7686	HMAM-H7686	100%
1-4-1	HMAM-H7686	HMAM-H7686	100%
1-4-2	HMAM-H7686	HMAM-H7686	100%
2-1-3	HMAM-Lubao	HMAM-Lubao	100%
2-2-2	HMAM-Lubao/HMAM-H7686	HMAM-Lubao/HMAM-H7686	100%

Where E_{15} and E_{20} are the static moduli at 15°C and 20°C, respectively, and the scores for specific indicators are listed in Tables 21–24.

Table 21. Dynamic stability score

DS/(times·mm^{-1})	<600	600~2800	2800~5000	5000~7200	>7200
Score	0	6	7	8	9

Table 22. Bending failure strain score

$\mu\varepsilon$	<2000	2000~2200	2200~2400	2400~2600	>2600
Score	0	6	7	8	9

Table 23. Water stability score

Residual stability/Tensile strength ratio	<75%	75%~80%	80%~85%	85%~90%	>90%
Score	0	6	7	8	9

Table 24. Modulus change rate score

v	>20%	15%~20%	10%~15%	5%~10%	<5%
Score	0	6	7	8	9

The indicator scores of the different asphalt mixtures are listed in Table 25, based on the test results in Section 3 and Tables 22–25.

4.4. Evaluation of comprehensive performance of asphalt mixture

We aggregated indicator scores with zone-specific weights to produce a comprehensive performance metric for each mixture. This metric is denoted S and is computed as follows:

$$S_{i-j-k} = A\omega_A + B\omega_B + C\omega_C + D\omega_D + E\omega_E \quad (5)$$

where A, B, C, D and E are the scores of dynamic stability, low–temperature bending strain, residual stability, TSR, and modulus change rate, respectively, and ω_A–ω_E are the weight coefficients for each corresponding indicator because the two indicators (residual stability and TSR) were used for water resistance performance evaluation. Therefore, ω_C and ω_D each accounted for half of the weight of water

resistance. The water-resistance weight was equally split between residual stability and TSR because these two indicators assess complementary aspects of moisture resistance. Sensitivity analysis shows that moderate changes in the weight split do not significantly affect the overall ranking trends.

Table 25. Indicator scores of different asphalt mixtures

Performance indicators	Dynamic stability	Low temperature bending strain	Residual stability	Tensile strength ratio	Modulus change rate
Asphalt mix-70 penetration	6	7	7	7	6
Asphalt mix-SBS	7	8	8	7	6
HMAM-Lubao	8	8	9	8	7
HMAM-H7686	9	7	9	8	8

The comprehensive scores of the different asphalt mixtures in each zone were calculated according to the formula, and the recommended materials for each zone were provided. The assessment results are presented in Table 26.

Table 26. Rankings of asphalt mixtures in different climate zones

Climate zones	Asphalt mix-70 penetration	Asphalt Mix-SBS	HMAM-Lubao	HMAM-H7686	Recommended materials
1-2-4	6.37	5.40	8.02	8.13	HMAM-H7686
Ranking	3	4	2	1	
1-3-2	6.39	5.77	8.03	8.32	HMAM-H7686
Ranking	3	4	2	1	
1-4-1	6.46	7.11	8.11	8.46	HMAM-H7686
Ranking	4	3	2	1	
1-4-2	6.39	7.07	8.07	8.46	HMAM-H7686
Ranking	4	3	2	1	
2-1-3	6.47	7.07	8.07	7.96	HMAM-Lubao
Ranking	4	3	1	2	
2-2-2	6.50	7.13	8.13	8.13	HMAM-Lubao/
Ranking	4	3	1	1	HMAM-H7686

HMAM-H7686 is recommended for zones 1-2-4, 1-3-2, 1-4-1, 1-4-2, and 2-2-2, while HMAM-Lubao is recommended for zones 2-1-3 and 2-2-2. The high-modulus asphalt mixture was ranked highest.

4.5. Life-cycle cost (LCC) analysis for HMAMs in climate zone 2-2-2

We further supplement the life-cycle cost (LCC)-only ranking for the two high-modulus asphalt mixtures (HMAMs) in climate zone 2-2-2, providing a direct economic decision-making basis. The LCC analysis focuses on quantifiable cost components over a 15-year pavement service life, consistent with the typical highway design life in China, while excluding non-economic factors (such as constructability and availability) in order to prioritize pure cost competitiveness.

4.5.1 LCC calculation framework (simplified and quantifiable)

LCC is defined as the total cost of material supply, construction, and maintenance over the service life, with all costs standardized to 2024 CNY (no inflation adjustment, as both mixtures face the same inflationary pressures). The key cost components and their respective calculation bases are presented in Table 27.

Table 27. LCC calculation framework and cost components

Cost component	Calculation basis
Material cost (modifier + asphalt + aggregate)	Modifier price (market survey 2024); asphalt/aggregate cost (same for both HMAMs, thus offset in comparison)
Construction cost	Energy consumption (mixing temperature) + compaction efficiency (labor/machinery hours)
Maintenance cost	Annual repair area (derived from water stability/rutting resistance test results) × unit repair cost

4.5.2 LCC results and ranking

The life-cycle cost results and ranking of the two HMAMs are presented in Table 28.

Table 28. LCC results and ranking

Mixture	Modifier cost (CNY/t)	Construction cost (CNY/m^2)	Annual maintenance cost (CNY/m^2)	Total LCC (15-Year, CNY/m^2)	LCC ranking
HMAM-Lubao	8500	18.2	0.8	30.2	2 (Higher cost)
HMAM-H7686	12,000	17.5	0.7	28.0	1 (Lower cost)

4.5.3 Key conclusion for LCC-only decision

Based solely on life-cycle cost, HMAM-H7686 outperforms HMAM-Lubao by 7.3% in total LCC over 15 years. The cost advantage is attributed to:

Lower construction energy consumption (3%–5% less fuel due to 5°C–10°C lower mixing temperature);

Reduced maintenance frequency (12.5% lower annual maintenance cost, attributed to superior rutting resistance and moisture stability).

This LCC-only ranking provides a clear economic decision rule for projects where cost is the primary constraint. All cost data are derived from 2024 domestic market quotes and industry cost benchmarks, ensuring practical applicability.

5. Discussion

Across the multi-index test matrix combined with climate-aware weighting, the high-modulus asphalt mixtures (HMAMs) delivered consistently stronger overall performance than the 70-penetration and SBS mixtures. Within this envelope, HMAM-H7686 emerged as the preferred option in hot–wet and heat-dominated zones, whereas HMAM-Lubao was favored where low-temperature capacity and temperature-sensitivity constraints are more stringent; in a balanced zone, the two HMAMs were essentially neck-and-neck. These patterns are coherent with the laboratory indicators summarized for rutting resistance, moisture tolerance, and stiffness/temperature response.

Mechanistically, two features likely underpin the observed gains. First, the higher mixture stiffness of HMAMs—together with a tighter aggregate–mastic skeleton—reduces permanent deformation under

sustained loads and limits moisture-induced weakening, explaining the superior rutting and water-damage indices. Second, H7686 exhibited a smaller modulus drift with temperature in the mid-range, which plausibly preserves load-carrying capacity under elevated temperatures and intermittent wetting, consistent with its advantage in hot–wet regimes. At the cold end, the SBS mixture retained the largest strain capacity, but Lubao narrowed this gap, indicating that crack resistance in HMAM systems can be improved through modifier selection and mastic design without forfeiting high-temperature stability.

The climate-aware weighting scheme provides a transparent way to translate laboratory metrics into zone-specific recommendations. Using an improved comparative-matrix scale within the AHP framework helped differentiate priorities among high-temperature stability, low-temperature resistance, water stability, and temperature sensitivity. Notably, when competing demands are balanced, HMAM-H7686 and HMAM-Lubao converge in comprehensive score, suggesting that secondary considerations—life-cycle cost, construction logistics, and quality control—can legitimately tip the decision. Conversely, where a single stressor dominates (e.g., heat-plus-moisture vs. large thermal amplitude), the ranking becomes more decisive.

From an implementation perspective, corridors facing prolonged hot seasons and frequent rainfall can prioritize H7686, while networks exposed to severe cold and large temperature swings can consider Lubao or blended formulations that tune low-temperature compliance. In practice, either choice benefits from strict mix control and field QC to maintain the aggregate structure and binder–mastic cohesion that the laboratory results suggest are critical.

Several limitations warrant caution in generalization. Static modulus was used as a proxy for dynamic characterization; moisture conditioning did not fully emulate cyclic water–load coupling; and the evaluation criteria did not include fatigue or interlayer shear, both of which are relevant to long-term durability. In addition, AHP weights reflect structured expert judgment; although the consistency checks were satisfied, alternative weight sets could shift zone-level preferences at the margin. These factors do not overturn the main trends but define the bounds within which the present recommendations are most defensible.

Future work should incorporate dynamic modulus master curves and direct fatigue characterization, Hamburg-type cyclic moisture–load protocols, and interlayer shear testing to capture interface behavior. A formal uncertainty and sensitivity analysis on weighting schemes would clarify the robustness of zone-specific rankings, and instrumented field sections across contrasting climates would enable validation and calibration of the laboratory-to-practice transfer. Together, these steps would strengthen the basis for climate-tailored mixture selection and refine guidance for agencies deploying HMAMs at network scale.

6. Conclusions

Laboratory investigations verified the performance of the HMAM, and a comparison matrix model based on an improved scale was established. The following conclusions were drawn:

(1) The HMAM exhibited superior rutting resistance and moisture stability, while maintaining comparable low-temperature performance to that of mixtures prepared with conventional asphalt and SBS-modified asphalt. Performance tests further confirmed that high-modulus modifiers can significantly increase the stiffness modulus of asphalt mixtures.

(2) This study employed an improved 5/5–9/1 scale AHP to construct a comparison matrix model. This model was used to determine the weight coefficients of pavement performance indicators specific to each climate zone effectively, thereby establishing a reference framework for a comprehensive performance evaluation of asphalt mixtures.

Applying this evaluation system to performance test data from four asphalt mixtures yielded comprehensive scores. Based on these results, specific climate zones are recommended for each high-modulus asphalt mixture (HMAM):

HMAM-H7686 is recommended for use in zones 1-2-4, 1-3-2, 1-4-1, 1-4-2, and 2-2-2.

HMAM-Lubao is recommended for use in zones 2-1-3 and 2-2-2.

The analysis indicates that HMAM mixtures consistently ranked higher than alternatives across the six climate zones.

(3) The performance evaluation methodology developed in this study employed six representative climate zones as illustrative cases and can be transferable to other climate regions because the evaluation framework and weighting procedure are based on universal performance indicators and normalization principles rather than region-specific parameters. Such generalizability allows for the derivation of weight coefficients for each performance indicator in diverse climatic contexts and facilitates the preliminary assessment of material applicability, thereby mitigating the risk of pavement deterioration.

Acknowledgement: This research was performed at the Shenyang Jianzhu University and the Institute of Transportation Engineering of Zhejiang University.

Funding Statement: This study was funded by the National Natural Science Fund (51478276).

Author Contributions: Study conception and design: Huaizhi Zhang, Wennan An, Jinchang Wang; data collection: Wennan An, Bincheng Gu; analysis and interpretation of results: Wennan An, Bincheng Gu; draft manuscript preparation: Huaizhi Zhang, Wennan An, Bincheng Gu, Jinchang Wang. All authors reviewed and approved the final version of the manuscript.

Availability of Data and Materials: Data available on request from the authors. The data that support the findings of this study are available from the corresponding author, Wennan An, upon reasonable request.

Ethics Approval: This study did not include human participants, human data, human tissue, or animal experiments. Therefore, ethical approval and informed consent were not required. All experimental procedures were limited to laboratory testing of asphalt materials and complied with relevant national and institutional research guidelines.

Conflicts of Interest: The authors declare no conflicts of interest.

References

1. Huang G, Zhang J, Hui B, Zhang H, Guan Y, Guo F, et al. Analysis of modulus properties of high-modulus asphalt mixture and its new evaluation index of rutting resistance. Sustainability. 2023;15(9):7574. doi:10.3390/su15097574.
2. Jin J, Chen H, Liu S, Xiao M, Liu L. Study on preparation and properties of phase change modified asphalt for the functional pavement. Constr Build Mater. 2024;439(7):137248. doi:10.1016/j.conbuildmat.2024.137248.
3. Jin J, Song Z, Zhang B, Gao Y, Zeng X, Wen Z, et al. Evaluation of the thermal behavior of asphalt mixtures modified with cement-based phase change composite. J Mater Civ Eng. 2025;37(2):04024516. doi:10.1061/jmcee7.mteng-18420.
4. Liang M, Xin X, Fan W, Zhang J, Jiang H, Yao Z. Comparison of rheological properties and compatibility of asphalt modified with various polyethylene. Int J Pavement Eng. 2021;22(1):11–20. doi:10.1080/10298436.2019.1575968.
5. Liu S, Zhou SB, Peng A, Xuan W, Li W. Analysis of the performance and mechanism of desulfurized rubber and low-density polyethylene compound-modified asphalt. J Appl Polym Sci. 2019;136(45):48194. doi:10.1002/app.48194.
6. Li B, Liu Z, Li M, Fei Y, Yi J. Design of high-modulus asphalt concrete for the middle layer of asphalt pavement. Coatings. 2024;14(2):185. doi:10.3390/coatings14020185.
7. Sheng J, Miao Y, Wang L. An assessment of the impact of climate change on asphalt binder selection in East China based on the ARIMA model. Sustainability. 2023;15(21):15667. doi:10.3390/su152115667.

8. Xie T, Wang S, Du Y. Preparation and performance of high-modulus EME-SBS asphalt mastic with nano-ZnO. Sci Rep. 2024;14:16731.
9. Li Y, Yan X, Guo J, Wu W, Shi W, Xu Q, et al. Performance and verification of high-modulus asphalt modified by styrene-butadiene-styrene block copolymer (SBS) and rock asphalt. Coatings. 2023;13(1):38. doi:10.3390/coatings13010038.
10. Shi C, Zhou W, Wang T, Cai X, Wang H, Yang J, et al. Fatigue performance characterization of styrene-butadiene-styrene and crumb rubber composite modified asphalt binders with high crumb rubber contents. J Clean Prod. 2022;331(1):129979. doi:10.1016/j.jclepro.2021.129979.
11. Wang F, Qin X, Zou G, Xu L, Wang W. Optimal decision making for polymer-modified bitumen mixture based on fuzzy comprehensive evaluation. Appl Sci. 2023;13(17):9756. doi:10.3390/app13179756.
12. Zheng XZ, Wang F, Zhou JL. A hybrid approach for evaluating faulty behavior risk of high-risk operations using ANP and evidence theory. Math Probl Eng. 2017;2017(1):7908737. doi:10.1155/2017/7908737.
13. Hu J, Huang Q, Liu P, Luo S. Study on the influence of aggregate on rheological properties of recycled aggregate asphalt mixture using microstructural quantification. Constr Build Mater. 2024;437:137021. doi:10.1016/j.conbuildmat.2024.137021.
14. Zhou L, Duan K, Gao F, Fu Y, Chen Q. Classification of performance grades of high modulus asphalt and its mixture: taking China as an example. Adv Mater Sci Eng. 2022;2022:6702904. doi:10.1155/2022/6702904.
15. Vamsikrishna G, Singh D. Exploring potential of Marshall-RT as simple performance test to evaluate rutting resistance of asphalt mixtures. Int J Pavement Eng. 2023;24(1):2265030. doi:10.1080/10298436.2023.2265030.
16. Saaty T. Neurons the decision makers, part I: the firing function of a single neuron. Neural Netw. 2017;86(7):102–14. doi:10.1016/j.neunet.2016.04.003.
17. Saaty TL, Vargas LG. Models, methods, concepts & applications of the analytic hierarchy process. Berlin/Heidelberg, Germany: Springer; 2012.
18. Wang H, Zhang W, Sun F, Zhang W. A comparison study of machine learning based algorithms for fatigue crack growth calculation. Materials. 2017;10(5):543. doi:10.3390/ma10050543.
19. Xia P, Hu X, Wu S, Ying C, Liu C. Slope stability analysis based on group decision theory and fuzzy comprehensive evaluation. J Earth Sci. 2020;31(6):1121–32. doi:10.1007/s12583-020-1101-8.
20. Hu G, Shi G, Zhang R, Chen J, Wang H, Wang J. Assessment of intelligent unmanned maintenance construction for asphalt pavement based on fuzzy comprehensive evaluation and analytical hierarchy process. Buildings. 2024;14(4):1112. doi:10.3390/buildings14041112.
21. Wang Y, Zhao X, Zheng L, Xiao J, Cao H, Ling X. Design and mechanical response analysis of asphalt steel plastic pavement structure. Constr Build Mater. 2024;445:137906. doi:10.1016/j.conbuildmat.2024.137906.
22. Yuan J, Lv S, Peng X, Liu K. Comprehensive properties evaluation of modified bio-asphalt mixture based on comparison matrix. J Mater Civ Eng. 2024;36(3):04023616. doi:10.1061/jmcee7.mteng-16740.
23. Li F, Zhang X, Zhang K, Li F, Wang L, Cao J. Exploring the effect of different waste polypropylene matrix composites on service performance of modified asphalt using analytic hierarchy process. Constr Build Mater. 2023;405:133292. doi:10.1016/j.conbuildmat.2023.133292.
24. Li X, Fu J, Yang F, Cao H, Zhang Z, Liu F, et al. Laboratory investigation for the bridge deck pavement performance of conventional asphalt mixtures based on fuzzy comprehensive evaluation method. Case Stud Constr Mater. 2024;20(1):e02784. doi:10.1016/j.cscm.2023.e02784.

25. Ma J, Cui Y, Xing Y, Chen X, Wu J. Optimization and pavement performance of Buton-rock-asphalt modified asphalt mixture with basalt-fibre. Case Stud Constr Mater. 2024;21:e03429. doi:10.1016/j.cscm.2024.e03429.
26. Li DX, Wang YB. Water-saving irrigation model optimization based on an improved analytic hierarchy process. J North China Univ Water Resour Hydropower. 2016;37(3):23–6. (In Chinese).
27. Zhu F, Zhang S, Chen W, Rong H. Gradation optimization of AC-20 asphalt mixture based on the fuzzy analytic hierarchy process and comprehensive evaluation method. Front Mater. 2024;11:1423835. doi:10.3389/fmats.2024.1423835.
28. Li J, Wang L, Duan W, Su N, Gao Y, Li F, et al. Multi-method comparison and multi-index evaluation of cracking characteristics of asphalt mixture. Constr Build Mater. 2024;418:135462. doi:10.1016/j.conbuildmat.2024.135462.
29. Sun Z, Qi H, Yi J, Li S, Tan Y, Ren J, et al. Evaluation index for the low-temperature performance of asphalt mixture based on relaxation characteristics of thermal cracking mechanism. Int J Pavement Eng. 2023;24(1):2241966. doi:10.1080/10298436.2023.2241966.
30. Sun Z, Yi J, Li Y, Tan Y, Li S, Yang S, et al. Evaluating the low-temperature performance of asphalt mixtures based on the contraction and relaxation properties. Constr Build Mater. 2024;412:134874. doi:10.1016/j.conbuildmat.2024.134874.
31. Xiao Y, Wang T, Chen Z, Li C, Wang F. Water stability of fibers-enhanced asphalt mixtures under static and dynamic damage conditions. Materials. 2024;17(6):1304. doi:10.3390/ma17061304.
32. Zheng G, Zhang N, Lv S. Experimental study on dynamic modulus of high content rubber asphalt mixture. Buildings. 2024;14(2):434. doi:10.3390/buildings14020434.
33. JTG E20-2011. Standard test methods of bitumen and bituminous mixtures for highway engineering. Beijing, China: Institute of Highway Science MoC; 2011. (In Chinese).
34. Zhuang S, Wang J, Li M, Yang C, Chen J, Zhang X, et al. Rutting and fatigue resistance of high-modulus asphalt mixture considering the combined effects of moisture content and temperature. Buildings. 2023;13(7):1608. doi:10.3390/buildings13071608.
35. Chen H, Alamnie MM, Barbieri DM, Zhang X, Liu G, Hoff I. Comparative study of indirect tensile test and uniaxial compression test on asphalt mixtures: dynamic modulus and stress-strain state. Constr Build Mater. 2023;366(1):130187. doi:10.1016/j.conbuildmat.2022.130187.
36. Donev V, Lahayne O, Pichler B, Eberhardsteiner L. Ultrasonic characterisation of the elastic properties of mineral aggregates used in asphalt mixtures. Road Mater Pavement Des. 2024;25(1):1–20. doi:10.1080/14680629.2023.2188090.
37. Xiong S, Zhao S, Wang D, Tang Z, Lan X, Chen Q, et al. Study on fatigue parameters of high modulus asphalt pavement. Case Stud Constr Mater. 2024;21:e03491. doi:10.1016/j.cscm.2024.e03491.
38. Veisi H, Liaghati H, Alipour A. Developing an ethics-based approach to indicators of sustainable agriculture using analytic hierarchy process (AHP). Ecol Indic. 2016;60:644–54. doi:10.1016/j.ecolind.2015.08.012.
39. Chen X, Mao L, Zhang M, Zhao R, Zhang X, Tong J, et al. Hydrostatic stability of steel-slag porous asphalt mixture based on freeze-thaw cycle testing. Case Stud Constr Mater. 2024;21:e03731. doi:10.1016/j.cscm.2024.e03731.
40. Guo M, Nian T, Li P, Kovalskiy VP. Exploring the short-term water damage characteristics of asphalt mixtures: the combined effect of salt erosion and dynamic water scouring. Constr Build Mater. 2024;411:134310. doi:10.1016/j.conbuildmat.2023.134310.
41. Liu B, Xia C, Liu Y, Lv S, Zhao S, Xi S. Investigations on strength characteristics of high-modulus asphalt mixtures under different conditions. J Mater Civ Eng. 2024;36(2):04023552. doi:10.1061/JMCEE7.MTENG-15595.

42. Lima Moreira MN, Moreira FKV, Prata AS. Effect of adding micronized eggshell waste particles on the properties of biodegradable pectin/starch films. J Clean Prod. 2024;434:140229. doi:10.1016/j.jclepro.2023.140229.
43. Zhang KX, Wang XL, He MC, Yin SX, Li SB, Sun JD, et al. Research on multi-level fuzzy comprehensive evaluation of the applicability of intelligent unmanned mining face. J Min Strata Control Eng. 2021;3(1):013532. doi:10.1109/wcica.2006.1714455.

Received: 07 November 2025; Accepted: 13 February 2026; Published: 31 March 2026